

The origin of domes on Europa: The role of thermally induced compositional diapirism

Robert T. Pappalardo and Amy C. Barr

Laboratory for Atmospheric and Space Physics, University of Colorado, Boulder, Colorado, USA

Received 1 December 2003; accepted 8 December 2003; published 9 January 2004.

[1] The surface of Jupiter's moon Europa is peppered by topographic domes, interpreted as sites of intrusion and extrusion. Diapirism is consistent with dome morphology, but thermal buoyancy alone cannot produce sufficient driving pressures to create the observed dome elevations. Instead, diapirs may initiate by thermal convection that induces compositional segregation. Exclusion of impurities from warm upwellings allows sufficient buoyancy for icy plumes to create the observed surface topography, provided the ice shell has a small effective elastic thickness (~ 0.2 to 0.5 km) and contains low-eutectic-point impurities at the few percent level. This model suggests that the ice shell may be depleted in impurities over time. **INDEX TERMS:** 5430 Planetology: Solid Surface Planets: Interiors (8147); 5455 Planetology: Solid Surface Planets: Origin and evolution; 6218 Planetology: Solar System Objects: Jovian satellites. **Citation:** Pappalardo, R. T., and A. C. Barr (2004), The origin of domes on Europa: The role of thermally induced compositional diapirism, *Geophys. Res. Lett.*, *31*, L01701, doi:10.1029/2003GL019202.

1. Dome Morphologies and Origins

[2] Galileo images show that subcircular to elliptical pits, spots, and domes (commonly referred to as "lenticulae") comprise Europa's mottled terrain [Carr *et al.*, 1998]. A range of sizes is observed [Greenberg *et al.*, 2003], but observational evidence suggests a preferred effective diameter of ~ 10 km [Spaun, 2001]. It is commonly considered that lenticulae are formed by diapirism related to solid-state convection within Europa's ice shell [Pappalardo *et al.*, 1998], potentially along with partial melting and disaggregation of the icy lithosphere [Head and Pappalardo, 1999; Collins *et al.*, 2000]. Models of icy volcanism [Fagents, 2004] and complete melt-through of Europa's icy shell [Carr *et al.*, 1998; Greenberg *et al.*, 1999] also have been suggested. Here we consider morphological and geophysical constraints on the origin of Europa's domes (Figure 1). We develop a model in which diapirism is initiated by thermal convection, which triggers compositional segregation within an impure ice shell, creating sufficient buoyancy to form domes (Figure 2).

[3] From initial Galileo high resolution image data, Carr *et al.* [1998] classified Europa's domes into two endmember types based on their relationships to preexisting terrain. Type 1 domes consist of material texturally distinct from the ridged plains, and typically of lower albedo (Figure 1a and 1b). Photoclinometric studies indicate heights of ~ 40 to 100 m [Fagents, 2004]. Embayment relationships and the

contrast in texture and morphology compared to the surrounding ridged plains indicates that older terrain has been destroyed and/or obscured by newer material during formation. Type 2 domes show preexisting terrain preserved on their surfaces (Figure 1c–1f), implying that the older surface has been upwarped but not destroyed. These intrusive domes have a mean diameter ~ 7 km [Spaun, 2001], and shading suggests similar heights to Type 1 domes. Fractures are observed along the crests of some (Figures 1c, 1e, and 1f). The boundaries of Type 2 domes can be continuous with respect to the surrounding terrain producing a convex form (Figure 1c), or they can have a more abruptly kinked boundary producing a relatively flat-topped form (Figure 1d). Alternatively, they can be bounded by abrupt scarps that are presumably tectonic (Figure 1e, western and eastern boundaries, and Figure 1f, western and northern boundaries), producing a relatively flat-topped or tilted form.

[4] The size similarity and morphological gradation among Type 1 and Type 2 domes argues that any comprehensive formation model should account for the characteristics of both types. Type 1 dome morphologies are analogous to terrestrial silicate magma domes [Fagents, 2004]. Diapiric material, which has pierced the overlying material as it has risen buoyantly through the subsurface, can extrude to produce analogous bun-shaped domes, in a manner similar to terrestrial salt diapirs [Talbot and Jarvis, 1984]. Extrusion of diapirs, along with partial melting and in situ degradation of near-surface material, may account for observed Type 1 dome morphologies.

[5] Diapirs can stall in the shallow subsurface (Figure 2), flexing or faulting the surface upward in the manner of laccoliths that forcibly bend or fault their overburden upward. Intrusions can create anticlinal convex or kinked surface structures as axisymmetric bending folds, or can punch their overburden upward along peripheral faults [Corry, 1988]. Fault failure occurs primarily at the peripheries and secondarily along the crests of laccolithic intrusions, where stresses are greatest [Pollard and Johnson, 1973]. Type 2 domes are an excellent match to the expected surface expression of laccolith-like intrusions, based on their subcircular planforms, variety of cross-sectional shapes (convex, kinked, punched), and peripheral and crestal failure.

2. Modelling Dome Formation

2.1. Intrusion Model

[6] The plate bending treatment of Pollard and Johnson [1973], developed to explain volcanic intrusive bodies, can be applied to diapiric intrusions that stall in Europa's shallow subsurface (e.g., beneath its cold brittle lithosphere). The maximum height w_0 of an elastic overburden

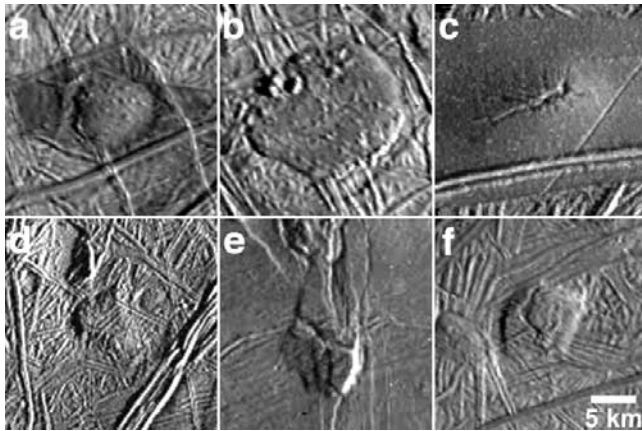


Figure 1. Examples of domes on Europa. (a–b) Type 1 (extrusive) domes; (c–f) Type 2 (intrusive) domes in (c) convex, (d) kinked, and (e, f) punched forms. North is to the top and illumination is from the right.

of effective thickness T_e domed upward by a driving pressure P_d uniformly distributed along a radius a , is

$$w_0 = \frac{3 P_d a^4}{16 B T_e^2} \quad (1)$$

where the elastic modulus $B = E/(1 - \nu^2)$, E is Young's modulus, and ν is Poisson's ratio. For ice at temperatures appropriate to Europa, $\nu \approx 0.33$ and $E \sim 1$ to 10 GPa [Mellor, 1986; Nimmo *et al.*, 2003a]. Flexural signatures have been used to infer $T_e \approx 0.1$ to 0.5 km in regions of severe local deformation assuming E values in the range above [Williams and Greeley, 1998; Billings and Kattenhorn, 2002]. Actual brittle lithospheric thickness will be greater than the effective thickness.

[7] Figure 3 plots the w_0 versus P_d , assuming a nominal Type 2 dome diameter $2a = 7$ km. To create these domes, diapiric intrusions could arch an ice overburden of $T_e \approx 0.1$ to 1 km to significant height if $P_d \sim 10^4$ to 10^7 Pa, depending on specific values of E and T_e . For larger radius intrusions (e.g., Figure 1c), equation (1) indicates that a given dome height can be made with lesser P_d .

2.2. Thermal Buoyancy

[8] Thermal diapirism has been proposed as a source of buoyancy for forming Europa's domes [Pappalardo *et al.*, 1998]. Solid-state convection can bring warm material to shallow (several km) depths within Europa's ice shell [Barr and Pappalardo, 2003]; however, stresses due to thermal convection are small. The maximum convective stress is

$$P_d \sim 0.1 \rho_i g \alpha \Delta T D \quad (2)$$

[McKinnon, 1998], where ρ_i is ice density, g is gravity, α is the coefficient of thermal expansion, ΔT is the temperature difference across the ice shell, and D is ice shell thickness. For $g = 1.3 \text{ m s}^{-2}$, $\alpha = 10^{-4} \text{ K}^{-1}$, and $\Delta T = 160 \text{ K}$, then $P_d \sim 4 \times 10^4 \text{ Pa}$ for a nominal ice shell thickness of $D \approx 20 \text{ km}$. This P_d cannot make Type 2 domes of significant height (Figure 3), unless T_e and E are very small; alternatively, D must be very large ($\sim 100 \text{ km}$) to generate significant uplift. Thermal upwellings are typically $\sim 0.1(\Delta T)$ warmer than their surroundings, creating density differences $\sim 0.1 \rho_i \alpha \Delta T$, or $\sim 1.5 \text{ kg m}^{-3}$. Modeling of Newtonian thermal

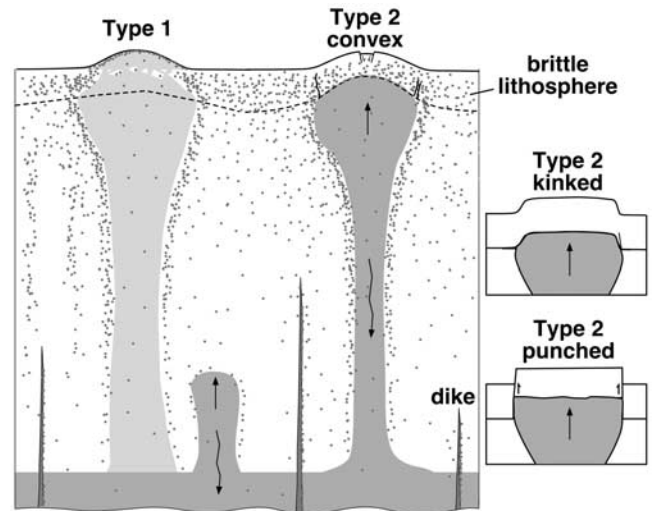


Figure 2. Schematic illustration of thermally induced compositional diapirism. As warm ice (dark gray) rises from the base of the ice shell, it melts overlying low-eutectic contaminants (stipples) and brines drain downward (squiggled arrows). This allows compositional buoyancy to aid diapiric rise. Extrusion creates a Type 1 dome, and intrusion can create Type 2 domes that are convex, kinked, or punched. Low-eutectic contaminant concentration is least in the warmest ice and locally concentrated around the diapirs from which they are expelled. Dome topography and subsurface compositional gradients persist after plumes have cooled (left, lighter gray) until subsequent ice flow redistributes the constituents. Diking might replenish some oceanic contaminants.

convection supports this analysis, predicting only $\sim 10 \text{ m}$ of relief above upwellings [Showman and Han, 2003].

[9] Diffusive cooling can cause diapirs to stall in the subsurface [Rathbun *et al.*, 1998]. If warm diapirs do reach the surface, thermal diffusion causes domes to relax as they cool [Nimmo and Manga, 2002] if not supported by dynamic processes or compositional density variations. Diapirs might concentrate tidal heating [Sotin *et al.*, 2002], perhaps allowing their rise to continue toward the surface; however, this model is uncertain because the scale of diapirs is much smaller than the length scale of tidal flexing [Moore, 2001].

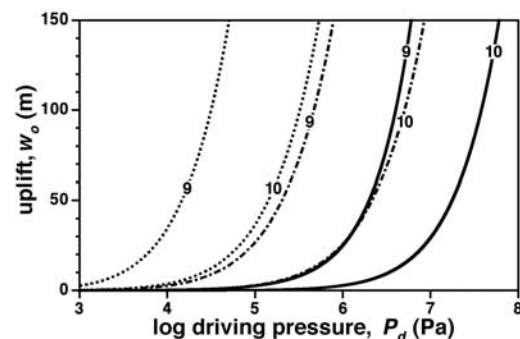


Figure 3. Maximum height w_0 of intrusive (Type 2) domes as a function of P_d , assuming a dome diameter $2a = 7$ km. Curves are for effective elastic thickness $T_e = 0.2$ km (dotted), 0.5 km (dot-dash), and 1 km (solid), for Young's modulus E values of 10^9 and 10^{10} Pa (labeled as $\log E$).

2.3. Compositional Buoyancy

[10] Differences in impurity levels are a potential source of compositional buoyancy to drive diapirism, and may be relevant to dome formation (Figure 2). Results from the Galileo NIMS instrument indicate that non-ice materials, modeled as hydrated sulfate salts [McCord *et al.*, 1998] or sulfuric acid hydrate [Carlson *et al.*, 1999], correlate with Europa's low albedo regions. However, contaminant levels within the ice are highly uncertain, because non-ice materials can become concentrated at the surface by thermal segregation or chemically altered by particle bombardment.

[11] A vigorously convecting icy shell is expected to have a nearly isothermal adiabatic temperature, T_{ad} , beneath a rigid stagnant lid. For basal heating, T_{ad} can be ~ 245 K [Barr and Pappalardo, 2003], while for an internally (tidally) heated ice shell, $T_{ad} \sim 250$ to 260 K [McKinnon, 1999; Nimmo and Manga, 2002]. The primary controls on T_{ad} —the activation energy of the ice flow law and the ocean temperature—are not expected to be significantly affected by impurities.

[12] Both sulfate and chloride contaminants are plausible constituents of Europa's icy shell [Kargel *et al.*, 2000]. Hydrated sulfate salts (including MgSO_4 , K_2SO_4 , and Na_2SO_4) have eutectic temperatures ~ 270 K (at 0.1 MPa) [Brass, 1980], securely above the predicted T_{ad} for Europa; therefore, these salts are expected to be stable against eutectic melting. In contrast, eutectic temperatures of hydrated chloride salts (including NaCl , KCl , CaCl_2 , and MgCl_2) are in the range ~ 220 to 250 K, less than or comparable to the expected T_{ad} . The ice- H_2SO_4 system has an extremely low eutectic of 211 K [Kargel *et al.*, 2000]. If hydrated chloride salts or sulfuric acid (herein collectively termed “low-eutectic” contaminants) exist within Europa's icy shell, they are expected to melt and produce brines in response to thermal convection. This should be the case throughout the warm base of the ice shell and wherever a warm ice plume contacts colder contaminant-rich ice.

[13] Melt is expected to drain through the ice at ~ 10 m yr^{-1} [Gaidos and Nimmo, 2000], faster than the ~ 0.1 to 1 m yr^{-1} vertical velocity of convective ice plumes [Barr and Pappalardo, 2003]. Therefore, warm plumes and the ice shell's warm base are expected to be relatively clean of low-eutectic impurities. A heterogeneous contaminant distribution is expected, superimposed on a gradient of decreasing low-eutectic impurity concentration with depth (Figure 2).

[14] The warmer ice of a rising diapir will be cleaner and thus buoyant relative to its surroundings. Figure 4 plots P_d due to a density difference $\Delta\rho$ between cleaner diapirs and the ambient icy shell, for a range of shell thicknesses. This $\Delta\rho$ can be expressed as a volume fraction ϕ of low-eutectic contaminants that melt and drain from warm plumes:

$$P_d = \phi(\rho_{le} - \rho_o)gD \quad (3)$$

where ρ_{le} is the average density of the low-eutectic solids and ρ_o is the ambient ice shell density. This relationship assumes simple isostasy above a column cleaned of low-eutectic contaminants through diapiric rise. We choose $\rho_o = 1000$ kg m^{-3} and $\rho_{le} = 1500$ kg m^{-3} , the latter representative of plausible low-eutectic contaminants such as $\text{H}_2\text{SO}_4 \bullet 8\text{H}_2\text{O}$ (1350 kg m^{-3}) and $\text{NaCl} \bullet 2\text{H}_2\text{O}$ (1610 kg m^{-3}). This implies $\phi \sim 2\%$ can produce $P_d \sim 10^5$ Pa for reasonable ice shell thicknesses (Figure 4). This is sufficient to upwarp Type 2 domes for intrusions beneath a brittle ice cover of $T_e \sim 0.2$ to

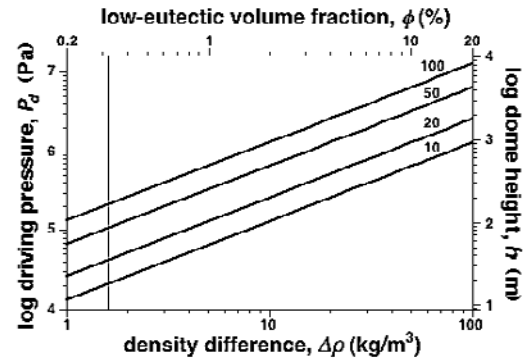


Figure 4. Driving pressure P_d available to upwarp intrusive domes, and neutral buoyancy height h of extrusive domes, as a function of compositional density difference $\Delta\rho$ and corresponding low-eutectic contaminant volume fraction ϕ , for a range of shell thicknesses D (labeled in km). Compositional buoyancy dominates over thermal for $\Delta\rho > 1.5$ kg m^{-3} (gray line), equivalent to $\phi > 0.3\%$.

0.5 km, depending on the specific value of E (Figure 3). The minor amounts of low-eutectic contaminants required are consistent with geochemical models of Europa's evolution [Kargel *et al.*, 2000]. For this ϕ , the latent heat attained from a diapir to melt low-eutectic contaminants would affect diapir temperatures by < 3 K.

[15] In a compositional buoyancy scenario, the height h of extrusive (Type 1) domes is expected to be the neutral buoyancy level of relatively clean diapiric ice compared to the ambient ice shell:

$$h = \Delta\rho D / (\rho_o - \Delta\rho). \quad (4)$$

If $\Delta\rho \ll \rho_o$ (valid for $\phi < 20\%$), this simplifies to $h = D\Delta\rho/\rho_o$, indicated on the right-hand axis of Figure 4. For $\phi = 2\%$, diapiric material can extrude to $h \approx 200$ m for $D = 20$ km, sufficient to create extrusive domes.

[16] In this model, low-eutectic contaminants may become depleted in Europa's ice shell over time. Diking may replenish oceanic contaminants near the base of the shell [Crawford and Stevenson, 1988], but this mechanism may not be relevant to its upper portions. Rather than assuming a steady-state, it is plausible that Europa's youthful surface age (~ 30 to 80 Myr [Zahnle *et al.*, 2003]) reflects the latest incarnation of an ice shell that is depleted in contaminants over time.

2.4. Double-Diffusive Analog

[17] Thermally-driven compositional segregation may be analogous to double-diffusive convection (DDC), in which both thermal and compositional gradients trigger fluid motions. DDC systems are governed by the thermal Rayleigh number

$$\text{Ra} = \rho g \alpha \Delta T D^3 / \kappa \eta \quad (5)$$

(where κ is thermal diffusivity, and η is viscosity), and a compositional Rayleigh number

$$\text{Ra}_c = \rho g \beta \Delta \phi D^3 / \kappa_c \eta \quad (6)$$

(where $\Delta\phi$ is the vertical composition gradient of low-eutectic contaminants across the ice shell, $\beta = [\rho_{le} - \rho_o]/\rho_o$, and κ_c is compositional diffusivity). In the “finger” regime, compositionally buoyant material rises in narrow upwel-

lings much smaller than the shell's thickness. This may be the case for Europa. The onset of the finger regime can be expressed as:

$$\kappa_c < \beta \Delta \phi \left[\frac{27\pi^4}{4} \frac{\eta}{\rho g D^3} + \frac{\alpha \Delta T}{\kappa} \right]^{-1} \quad (7)$$

[Kundu, 1990, p. 366]. For an ice shell viscosity $\eta = 10^{18}$ Pa s, thermal diffusivity $\kappa = 10^{-6}$ m² s⁻¹, and $D = 20$ km, convection in the finger regime occurs if $\kappa_c \leq 10^{-7}$ m² s⁻¹.

[18] We envision that compositional diffusion is governed by melt composition, drainage velocity, and a characteristic length scale for a European drainage channel. These parameters are poorly constrained, so we cannot draw firm conclusions regarding the behavior of Europa's ice shell. True DDC predicts that the system evolves toward a steady state, but here contaminants are depleted in the ice shell over time, so DDC serves only as a starting point for modelling relevant processes.

3. Summary and Implications

[19] The morphological characteristics of Europa's Type 1 and Type 2 domes can be accounted for by diapiric extrusion and intrusion, respectively. The required buoyancy is difficult to achieve through thermal convection alone but can be produced by percentage-level compositional differences between ice diapirs and their surroundings, if low-eutectic contaminants melt and drain from warm plumes and if the effective thickness of the brittle lithosphere is very small (~0.2 to 0.5 km). Compositional differences can also explain the topography of extrusive domes. Existence of both thermal and compositional gradients suggests that double-diffusive convection may be relevant to Europa's ice shell. Convection in the compositionally dominated finger regime could produce narrow diapirs.

[20] Thermally induced compositional buoyancy offers a comprehensive and geophysically plausible means for forming Europa's domes. An analogous model has been applied to Europa's bands by Nimmo *et al.* [2003b], and is potentially applicable to the satellite's larger chaos regions as well. The model implies compositional heterogeneity on a local scale within the ice shell, which might be detectable by future missions using ground penetrating radar. The process would allow deep interior material to breach Europa's cold brittle lithosphere, potentially transporting oceanic and astrobiologically relevant materials to the surface where they could be examined by spacecraft.

[21] **Acknowledgments.** We thank C. Sotin, an anonymous referee for helpful reviews, and W. B. Moore and J. Toomre for valuable discussion. This work was supported by NASA Exobiology NCC2-1340 and NASA GSRP NGT5-50337.

References

Barr, A. C., and R. T. Pappalardo (2003), Numerical simulation of non-Newtonian convection in ice: Application to Europa, in *Lunar Planet. Sci. Conf., XXXIV*, abstract # 1477, Lunar and Planetary Institute, Houston (CD-ROM).
 Billings, S. E., and S. A. Kattenhorn (2002), Determination of ice crust thickness from flanking cracks along ridges on Europa, in *Lunar Planet.*

Sci. Conf., XXXIII, abstract #1813, Lunar and Planetary Institute, Houston (CD-ROM).
 Brass, G. W. (1980), Stability of brines on Mars, *Icarus*, 42, 20–28.
 Carlson, R. W., R. E. Johnson, and M. S. Anderson (1999), Sulfuric acid on Europa and the radiolytic sulfur cycle, *Science*, 286, 97–99.
 Carr, M. H., *et al.* (1998), Evidence for a subsurface ocean on Europa, *Nature*, 391, 363–365.
 Collins, G. C., J. W. Head III, R. T. Pappalardo, and N. A. Spaul (2000), Evaluation of models for the formation of chaotic terrain on Europa, *J. Geophys. Res.*, 105(E1), 1709–1716.
 Corry, C. E. (1988), *Laccoliths: Mechanics of Emplacement and Growth*, Geol. Soc. of Am. Spec. Pap. 220, 110 pp.
 Crawford, G. D., and D. J. Stevenson (1988), Gas-driven water volcanism and the resurfacing of Europa, *Icarus*, 73, 66–79.
 Fagents, S. A. (2004), Considerations for effusive cryovolcanism on Europa: The post-Galileo perspective, *J. Geophys. Res.*, in press.
 Gaidos, E., and F. Nimmo (2000), Tectonics and water on Europa, *Nature*, 405, 637.
 Greenberg, R., G. V. Hoppa, B. R. Tufts, P. E. Geissler, and J. Reilly (1999), Chaos on Europa, *Icarus*, 141, 263–286.
 Greenberg, R., M. A. Leake, G. V. Hoppa, and B. R. Tufts (2003), Pits and uplifts on Europa, *Icarus*, 161, 102–126.
 Head, J. W., and R. T. Pappalardo (1999), Brine mobilization during lithospheric heating on Europa: Implications for formation of chaos terrain, lenticula texture, and color variations, *J. Geophys. Res.*, 104(E11), 27,143–27,155.
 Kargel, J. S., *et al.* (2000), Europa's crust and ocean: Origin, composition, and the prospects for life, *Icarus*, 148, 226–265.
 Kundu, P. (1990), *Fluid Mechanics*, Academic.
 McCord, T. B., *et al.* (1998), Hydrated salt minerals on Europa's surface from the Galileo NIMS investigation, *J. Geophys. Res.*, 104(E5), 11,827–11,851.
 McKinnon, W. B. (1998), Geodynamics of icy satellites, in *Solar System Ices*, edited by Schmitt *et al.*, pp. 525–550.
 McKinnon, W. B. (1999), Convective instability in Europa's floating ice shell, *Geophys. Res. Lett.*, 26(7), 951–954.
 Mellor, M. (1986), Mechanical behavior of sea ice, in *The Geophysics of Sea Ice*, edited by N. Untersteiner, New York: Plenum, pp. 165–281.
 Moore, W. B. (2001), Coupling tidal dissipation and convection, *Bull. Am. Astron. Assoc.*, 33, 1106.
 Nimmo, F., and M. Manga (2002), Causes, characteristics and consequences of convective diapirism on Europa, *Geophys. Res. Lett.*, 29(23), doi:10.1029/2002GL015754.
 Nimmo, F., B. Giese, and R. T. Pappalardo (2003a), Estimates of Europa's ice shell thickness from elastically-supported topography, *Geophys. Res. Lett.*, 30(5), 1233, doi:10.1029/2002GL016660.
 Nimmo, F., R. T. Pappalardo, and B. Giese (2003b), On the origins of band topography, Europa, *Icarus*, 166, 21–32.
 Pappalardo, R. T., *et al.* (1998), Geological evidence for solid-state convection in Europa's ice shell, *Nature*, 391, 365–368.
 Pollard, D. D., and A. M. Johnson (1973), Mechanics of growth of some laccolithic intrusions in the Henry Mountains, Utah, II: Bending and failure of overburden layers and sill formation, *Tectonophysics*, 18, 311–354.
 Rathbun, J. A., G. S. Musser Jr., and S. W. Squyres (1998), Ice diapirs on Europa: Implications for liquid water, *Geophys. Res. Lett.*, 25(22), 4157–4160.
 Showman, A. P., and L. Han (2003), Numerical simulations of convection in Europa's ice shell: Implications for surface features, in *Lunar Planet. Sci. Conf., XXXIV*, abstract #1806, Lunar and Planetary Institute, Houston (CD-ROM).
 Sotin, C. J., J. W. Head, and G. Tobie (2002), Europa: Tidal heating of upwelling thermal plumes and the origin of lenticulae and chaos melting, *Geophys. Res. Lett.*, 29(8), doi:10.1029/2001GL013844.
 Spaul, N. A. (2001), *Chaos, Lenticulae and Lineae on Europa*, Ph.D. thesis, Brown Univ.
 Talbot, C. J., and R. J. Jarvis (1984), Age, budget and dynamics of an active salt extrusion in Iran, *J. Struct. Geol.*, 6, 521–533.
 Williams, K. K., and R. Greeley (1998), Estimates of ice thickness in the Conamara Chaos region of Europa, *Geophys. Res. Lett.*, 25(23), 4273–4276.
 Zahnle, K., P. Schenk, H. F. Levison, and L. Dones (2003), Cratering rates in the outer solar system, *Icarus*, 163, 263–289.

R. T. Pappalardo and A. C. Barr, Laboratory for Atmospheric and Space Physics, University of Colorado, Boulder, CO 80309-0392, USA. (robert.pappalardo@colorado.edu)